INTERNATIONAL JOURNAL OF
NUMERICAL ANALYSIS AND MODELING
Volume 14, Number 4-5, Pages 500–510

FINITE ELEMENT METHOD TO CONTROL THE DOMAIN SINGULARITIES OF POISSON EQUATION USING THE STRESS INTENSITY FACTOR : MIXED BOUNDARY CONDITION

SEOKCHAN KIM AND HYUNG-CHUN LEE

Abstract. In this article, we consider the Poisson equation on a polygonal domain with the domain singularity raised from the changed boundary conditions with the inner angle $\omega > \frac{\pi}{2}$. The solution of the Poisson equation with such singularity has a singular decomposition: regular part plus singular part. The singular part is a linear combination of one or two singular functions. The coefficients of the singular functions are usually called stress intensity factors and can be computed by the extraction formula. In [11] we introduced a new partial differential equation which has 'zero' stress intensity factor using this stress intensity factor, from whose solution we can obtain a very accurate solution of the original problem simply by adding singular part. Although the method in [11] works well for the Poisson problem with Dirichlet boundary condition, it does not give optimal results for the case with stronger singularity, for example, mixed boundary condition with bigger inner angle. In this paper we give a revised algorithm which gives optimal convergences for both cases.

Key words. Finite element, singular function, dual singular function, stress intensity factor.

1. Introduction

Let Ω be an open, bounded polygonal domain in $\mathbb{R}^2$ and let Γ_D and Γ_N be a partition of the boundary of Ω such that $\partial\Omega = \overline{\Gamma}_D \cup \overline{\Gamma}_N$ and $\Gamma_D \cap \Gamma_N = \emptyset$. As a model problem, we consider the following Poisson equation with mixed boundary conditions:

$$(1) \qquad \left\{ \begin{array}{rcll} -\Delta u &=& f & \text{in } \Omega, \\ u &=& 0 & \text{on } \Gamma_D, \\ \frac{\partial u}{\partial \nu} &=& 0 & \text{on } \Gamma_N, \end{array} \right.$$

where $f \in L^2(\Omega)$, Δ stands for the Laplacian operator and ν denotes the outward unit vector normal to the boundary.

If $\Gamma_N = \emptyset$ and the domain is convex or smooth, we expect to have an optimal convergence rate with standard finite element method. But it is not true for Poisson problems defined on non-convex domains. The solution u of the Poisson equation with such singularity has a singular decomposition: $u = w + \lambda\eta s$, where $w \in H^2(\Omega) \cap H^1_D(\Omega)$, η is a smooth cut-off function and s is a singular function. Here, $H^1_D(\Omega) = \{u \in H^1(\Omega) : u = 0 \text{ on } \Gamma_D\}$.

Such lack of regularity affects the accuracy of the finite element approximation. There were several approaches in the literatures for overcoming this difficulty. One is based on local mesh refinement (see, e.g., [1, 13, 14, 15, 16] and references therein). The advantage of the method of local mesh refinement is that the knowledge of the exact forms of the singular functions is not needed. Another is done by augmenting the space of trial functions in which one looks for the approximate solution (see, e.g.,[2, 3, 4, 6, 7] and references therein). In [4], they introduced a new approach

Received by the editors December 1, 2016 and, in revised form, March 30, 2017.
1991 *Mathematics Subject Classification.* 65F10, 65N30.

that pose a partial differential equation with regular part of the solution, then compute the stress intensity factor and the solution.

The coefficient λ of the singular function is usually called stress intensity factor and can be computed by the extraction formula. In [11] we introduced a new partial differential equation which has 'zero' stress intensity factor, from whose solution we got accurate solution of the original problem simply by adding singular part.

Although the method in [11] works well for the Poisson problem with Dirichlet boundary condition, it does not give optimal results for the case with stronger singularity, for example, mixed boundary condition with bigger inner angle. In this paper we give a revised algorithm which gives an optimal convergence for both cases. In this paper we assume there is only one singular point raised from mixed Dirichlet and Neumann boundary condition.

We will use the standard notations and definitions for the Sobolev spaces $H^t(\Omega)$ for $t \geq 0$, and the associated inner products are denoted by $(\cdot,\cdot)_{t,\Omega}$, with their respective norms and seminorms are denoted by $\|\cdot\|_{t,\Omega}$ and $|\cdot|_{t,\Omega}$. The space $L^2(\Omega)$ is interpreted as $H^0(\Omega)$, in which case the inner product and norm will be denoted by $(\cdot,\cdot)_\Omega$ and $\|\cdot\|_\Omega$, respectively. However, we will omit Ω if there is no chance of misunderstanding.

In section 2 we give the forms of singular functions and the dual singular functions together with the extraction formula. In section 3 we suggest a revised algorithm and some theorems. In section 4 and 5 we give finite element approximation and some examples with numerical results.

2. Singular functions and extraction formula

We use a cut-off function to isolate the singular behavior of the problem. So, we first give the definition of the cut-off functions with parameters. Set

$$B(r_1;r_2) = \{(r,\theta):\ r_1 < r < r_2 \text{ and } 0 < \theta < \omega\} \cap \Omega \quad \text{and} \quad B(r_1) = B(0;r_1).$$

We define a family of cut-off functions of r as follows:

$$\eta_\rho(r) = \begin{cases} 1 & \text{in } B(\tfrac{1}{2}\rho), \\ \frac{15}{16}\left\{\frac{8}{15} - p(r) + \frac{2}{3}p(r)^3 - \frac{1}{5}p(r)^5\right\} & \text{in } \bar{B}(\tfrac{1}{2}\rho;\ \rho), \\ 0 & \text{in } \Omega \setminus \bar{B}(\rho), \end{cases} \tag{2}$$

where $p(r) = 4r/\rho - 3$. Here, ρ is a parameter which will be determined so that the singular part $\eta_\rho s$ has the same boundary condition as the solution u of the Model problem, s is the singular function which is given in (3)–(7). Note that $\eta_\rho(r)$ is C^2.

If $\Gamma_N = \emptyset$ with the inner angle $\omega, \pi < \omega < 2\pi$, as in [11], we have one singular function and its dual singular function:

$$s = s(r,\theta) = r^{\frac{\pi}{\omega}} \sin\frac{\pi\theta}{\omega} \quad \text{and} \quad s_- = s_-(r,\theta) = r^{-\frac{\pi}{\omega}} \sin\frac{\pi\theta}{\omega}. \tag{3}$$

If $\Gamma_N \neq \emptyset$ and the boundary condition changes its type at vertices with the inner angle ω, $\frac{\pi}{2} < \omega < 2\pi$, we have a list of the singular functions:

1) **D/N** If $\frac{\pi}{2} < \omega \leq \frac{3\pi}{2}$, there is a singular function of the form

$$s_1 = s_1(r,\theta) = r^{\frac{\pi}{2\omega}} \sin\frac{\pi\theta}{2\omega}; \tag{4}$$

If $\frac{3\pi}{2} < \omega < 2\pi$, there are two singular functions of the form

$$s_1 = s_1(r,\theta) = r^{\frac{\pi}{2\omega}} \sin\frac{\pi\theta}{2\omega} \quad \text{and} \quad s_3 = s_3(r,\theta) = r^{\frac{3\pi}{2\omega}} \sin\frac{3\pi\theta}{2\omega}; \tag{5}$$

2) **N/D** If $\frac{\pi}{2} < \omega \le \frac{3\pi}{2}$, there is a singular function of the form

$$s_1 = s_1(r,\theta) = r^{\frac{\pi}{2\omega}} \cos\frac{\pi\theta}{2\omega}; \tag{6}$$

If $\frac{3\pi}{2} < \omega < 2\pi$, there are two singular functions of the form

$$s_1 = s_1(r,\theta) = r^{\frac{\pi}{2\omega}} \cos\frac{\pi\theta}{2\omega} \quad \text{and} \quad s_3 = s_3(r,\theta) = r^{\frac{3\pi}{2\omega}} \cos\frac{3\pi\theta}{2\omega}. \tag{7}$$

Here, D/N and N/D mean that type of boundary conditions changes passing the singular point.

For convenience, we denote index set of singular functions by L:

$$L = \begin{cases} \{1\} & \text{for} \quad (4) \text{ and } (6), \\ \{1,3\} & \text{for} \quad (5) \text{ and } (7). \end{cases} \tag{8}$$

It is well known that the solution of problem (1) has the following singular function representation([4, 5]):

$$u = w + \sum_{j\in L} \lambda_j \eta s_j, \tag{9}$$

with $w \in H^2(\Omega) \cap H^1_D(\Omega)$. For the computation of the coefficient λ_j we need to use the so-called dual singular functions, for $j \in L$,

$$s_{-j} = s_{-j}(r,\theta) = r^{-\frac{j\pi}{2\omega}} \sin\frac{j\pi\theta}{2\omega} \quad \text{and} \quad s_{-j} = s_{-j}(r,\theta) = r^{-\frac{j\pi}{2\omega}} \cos\frac{j\pi\theta}{2\omega} \tag{10}$$

corresponding to

$$s_j = s_j(r,\theta) = r^{\frac{j\pi}{2\omega}} \sin\frac{j\pi\theta}{2\omega} \quad \text{and} \quad s_j = s_j(r,\theta) = r^{\frac{j\pi}{2\omega}} \cos\frac{j\pi\theta}{2\omega} \tag{11}$$

respectively. Note that $s_1 \in H^{\frac{\pi}{2\omega}-\epsilon}(\Omega)$ and $s \in H^{\frac{\pi}{\omega}-\epsilon}(\Omega)$ for any $\epsilon > 0$, so the singularity in the mixed case is much stronger.

The coefficient, λ_j, is called 'stress intensity factor' and can be computed by the following extraction formula (see [5, 7, 17]):

$$\lambda_j = \frac{2}{j\pi}\int_\Omega f\eta s_{-j}dx + \frac{2}{j\pi}\int_\Omega u\Delta(\eta s_{-j})dx. \tag{12}$$

Note that both s_j and s_{-j} are harmonic functions in Ω.

3. Algorithms and Theorems

In [11], we considered the Poisson problem with Dirichlet boundary condition with one domain singularity. i.e. we assumed $\Gamma_N = \emptyset$ and let V_h be the continuous piecewise linear finite element space and suggested the following Algorithm:

Alg 1.: find $u_h \in V_h$ such that

$$(\nabla u_h, \nabla v) = (f, v) \quad \forall\ v \in V_h. \tag{13}$$

Alg 2.: Then compute λ_h by

$$\lambda_h = \frac{1}{\pi}\int_\Omega f\eta s_- dx + \frac{1}{\pi}\int_\Omega u_h\Delta(\eta s_-)dx. \tag{14}$$

Alg 3.: find w_h such that $w_h + \lambda_h s \in V_h$ and

$$(\nabla w_h, \nabla v) = (f, v) \quad \forall\ v \in V_h. \tag{15}$$

Alg 4.: Then $u_h = w_h + \lambda_h s$.

Note that the first two steps are just the standard FEM and well-known extraction formula([2, 3]). The essence of the paper [11] is Alg 3-Alg 4, given approximated stress intensity factor, which give a regular solution of a weak problem associated with a partial differential equation with 'zero' stress intensity factor and the solution of the original equation.

In the case of Poisson problem with Dirichlet boundary condition the above algorithm works well (See [11]), but in the case of mixed boundary condition the results are not good enough. Here we remind that the accuracy of λ_h computed by the extraction formula depends on the accuracy of the solution u_h, which ultimately depends on the regularity of u (See [3]).

3.1. Algorithm. Naturally we pose an algorithm which apply the idea of A3-A4 more than once. Here is the adjusted Algorithm:

A1.: Find a solution $u^{(0)}$ of (1) and

A2.: compute the stress intensity factors $\lambda_j^{(0)}, j \in L$, from (12).

A3.: For $i = 1, 2, \cdots, N$;

A3-1.: Solve, for $w^{(i)}$,

$$\left\{ \begin{array}{rcll} -\Delta w^{(i)} &=& f & \text{in } \Omega, \\ w^{(i)} &=& -\sum_{j\in L} \lambda_j^{(i-1)} s_j & \text{on } \Gamma_D, \\ \frac{\partial w^{(i)}}{\partial \nu} &=& -\sum_{j\in L} \lambda_j^{(i-1)} \frac{\partial s_j}{\partial \nu} & \text{on } \Gamma_N. \end{array} \right. \tag{16}$$

A3-2.: Let $u^{(i)} = w^{(i)} + \sum_{j\in L} \lambda_j^{(i-1)} s_j$.

A3-3.: Compute $\lambda_j^{(i)}$ by

$$\lambda_j^{(i)} = \frac{2}{j\pi} \int_\Omega f \eta s_{-j} dx + \frac{2}{j\pi} \int_\Omega u^{(i)} \Delta(\eta s_{-j}) dx, \quad j \in L. \tag{17}$$

In the loop of **A3**, $N = 1$ is enough for the cases D/N or N/D with $\frac{\pi}{2} < \omega \le \frac{3\pi}{2}$ and cases D/D or N/N with any concave angle. Even for the more singular cases D/N or N/D with $\frac{3\pi}{2} < \omega < 2\pi$, $N = 2$ is enough.

3.2. Well-posedness. Consider the following partial differential equation.

$$\left\{ \begin{array}{rcll} -\Delta w &=& f & \text{in } \Omega, \\ w &=& -\sum_{j\in L} \lambda_j s_j & \text{on } \Gamma_D, \\ \frac{\partial w}{\partial \nu} &=& -\sum_{j\in L} \lambda_j \frac{\partial s_j}{\partial \nu} & \text{on } \Gamma_N. \end{array} \right. \tag{18}$$

The following theorems show (18) has a regular solution.

Theorem 3.1. *If* (1) *has a solution u as in* (9) *with the stress intensity factors $\lambda_j (j \in L)$, then* (18) *has a unique solution w in $H^2(\Omega)$.*

Proof. First, we note that (1) has a unique solution and its stress intensity factors are λ_j, $j \in L$. The uniqueness of the solution of Poisson problem also implies that the following equation has a unique solution, with the stress intensity factors $-\lambda_j$:

$$\left\{ \begin{array}{rcll} -\Delta p &=& 0 & \text{in } \Omega, \\ p &=& -\sum_{j\in L} \lambda_j s_j & \text{on } \Gamma_D, \\ \frac{\partial p}{\partial \nu} &=& -\sum_{j\in L} \lambda_j \frac{\partial s_j}{\partial \nu} & \text{on } \Gamma_N. \end{array} \right. \tag{19}$$

(Note that $p = -\sum_{j\in L} \lambda_j s_j$ is the unique solution and the coefficients of the singular function s_j are the stress intensity factors.) By adding the two equations,

(1) and (19), we have the following equation

$$
\left\{\begin{array}{rcll} -\Delta w & = & f & \text{in } \Omega, \\ w & = & -\sum_{j\in L}\lambda_j s_j & \text{on } \Gamma_D, \\ \frac{\partial w}{\partial \nu} & = & -\sum_{j\in L}\lambda_j \frac{\partial s_j}{\partial \nu} & \text{on } \Gamma_N, \end{array}\right. \tag{20}
$$

whose solution $w = u + p$ belongs to $H^2(\Omega)$. □

Theorem 3.2. *If λ_j is the stress intensity factors given by* (12) *with the solution u in* (1)*, and w is the solution of* (18)*, then $u = w + \sum_{j\in L}\lambda_j s_j$ is the unique solution of* (1).

Proof. We only need to show $u = w + \sum_{j\in L}\lambda_j s_j$ is the solution to (1) when w is the solution of (18). Since $\Delta s_j = 0$, we have

$$-\Delta u = -\Delta w - \sum_{j\in L}\lambda_j \Delta s_j = -\Delta w = f.$$

Moreover, we have

$$u|_{\Gamma_D} = w|_{\Gamma_D} + \sum_{j\in L}\lambda_j s_j|_{\Gamma_D} = -\sum_{j\in L}\lambda_j s_j + \sum_{j\in L}\lambda_j s_j = 0,$$

and

$$\frac{\partial u}{\partial \nu}|_{\Gamma_N} = \frac{\partial w}{\partial \nu}|_{\Gamma_N} + \sum_{j\in L}\lambda_j \frac{\partial s_j}{\partial \nu}|_{\Gamma_N} = 0.$$

□

Now we suggest an algorithm in variational form for the solution u of the model problem (1) :

V1.: find $u \in H^1_D(\Omega)$ such that

$$(\nabla u, \nabla v) = (f, v), \quad \forall\, v \in H^1_D(\Omega). \tag{21}$$

V2.: Then compute $\lambda_j^{(0)}$, $j \in L$, by (12) with u.
V3.: Do the following, for $i = 1, 2, \cdots, N$;
V3-1.: find $w^{(i)}$ such that $w^{(i)} + \sum_{j\in L}\lambda_j^{(i-1)} s_j \in H^1_D(\Omega)$ and

$$(\nabla w^{(i)}, \nabla v) = (f, v) - \sum_{j\in L}\lambda_j (\frac{\partial s_j}{\partial \nu}, v)|_{\Gamma_N}, \quad \forall\, v \in H^1_D(\Omega). \tag{22}$$

V3-2.: Set $u^{(i)} = w^{(i)} + \sum_{j\in L}\lambda_j^{(i-1)} s_j$.
V3-3.: Compute $\lambda_j^{(i)}$, $j \in L$, by (12) with $u^{(i)}$.

The existence and uniqueness of the solution u and w in **V1** and **V3-1** are clear([14]). By Theorem 3.1 and Theorem 3.2, we have that the solution $w \in H^2(\Omega)$, and that u is the solution of (1).

3.3. Comparision of the effectiveness of the algorithm. To compare the effectiveness of our algorithm to that of DSFM, we state the simplified DSFM algorithm as follows:

DSFM 1) Find the solution u of (1) using the standard finite element method.

DSFM 2) Compute the stress intensity factor λ_j, $j \in L$, using the extraction formula (12).

DSFM 3) Find the solution w

$$\left\{\begin{array}{rcll} -\Delta w &=& f + \sum_{j\in L} \lambda_j \Delta(\eta s_j) & \text{in } \Omega, \\ w &=& 0 & \text{on } \Gamma, \\ \frac{\partial u}{\partial \nu} &=& 0 & \text{on } \Gamma_N. \end{array}\right. \tag{23}$$

DSFM 4) Set $u = w + \sum_{j\in L} \lambda_j \eta s_j$.

Here, we note that although the algorithms used in [2, 3] are a little different from the above one, we just use this to emphasize that, in the DSFM-type algorithms, the input function is changed form f to $f + \sum_{j\in L} \lambda_j \Delta(\eta s_j)$.

Since the errors depend linearly on the L^2-norm of input functions, we may predict the error in the new algorithm is less than that of DSFM as we see in the following lemma.

Lemma 3.1. *If we assume Ω is a L-shape domain as in* **Example 1** *of* Chapter *5, and if $f \equiv 1$ in Ω, we have*

$$\|f + \lambda\Delta(\eta s)\| \approx 7.098 \quad \text{and} \quad \|f\| = \sqrt{3} \approx 1.732 \tag{24}$$

with $\lambda \approx 0.4019$.

Proof. See [11]. $\square$

4. Finite Element Approximation

In this section we present the standard finite element approximation for u and λ obtained in our algorithm in the L^2 and H^1 norms.

Let $\mathcal{T}_h$ be a partition of the domain Ω into triangular finite elements, i.e., $\Omega = \cup_{K\in\mathcal{T}_h} K$, with $h = \max\{\text{diam}K : K \in \mathcal{T}_h\}$. Let V_h be continuous piecewise linear finite element space; i.e.,

$$V_h = \{\phi_h \in C^0(\Omega) : \phi_h|_K \in P_1(K)\ \forall K \in \mathcal{T}_h, \phi_h = 0 \text{ on } \Gamma_{\mathrm{D}}\} \subset \mathrm{H}^1_{\mathrm{D}}(\Omega),$$

where $P_1(K)$ is the space of linear functions on K.

Now, we can find an approximated solution u_h using the following algorithm:

FEA1.: find $u_h^{(0)} \in V_h$ such that

$$(\nabla u_h^{(0)}, \nabla v) = (f, v), \quad \forall\ v \in V_h. \tag{25}$$

FEA2.: Then, compute $\lambda_{j,h}^{(0)}$ by

$$\lambda_{j,h}^{(0)} = \frac{2}{j\pi}\int_\Omega f\eta s_{-j} dx + \frac{2}{j\pi}\int_\Omega u_h^{(0)} \Delta(\eta s_{-j}) dx, \quad j \in L. \tag{26}$$

FEA3.: Do the followings, for $i = 1, 2, \cdots, N$;

FEA3-1.: find $w_h^{(i)}$ such that $w_h^{(i)} + \sum_{j\in L} \lambda_{j,h}^{(i-1)} s_j \in V_h$ and

$$(\nabla w_h^{(i)}, \nabla v) = (f, v) - \sum_{j\in L} \lambda_j (\frac{\partial s_j}{\partial \nu}, v)|_{\Gamma_N}, \quad \forall\ v \in V_h. \tag{27}$$

FEA3-2.: Set $u_h^{(i)} = w_h^{(i)} + \sum_{j\in L} \lambda_{j,h}^{(i-1)} s_j$.

FEA3-3.: Compute $\lambda_{j,h}^{(i)}$ by

$$\lambda_{j,h}^{(i)} = \frac{2}{j\pi}\int_\Omega f\eta s_{-j} dx + \frac{2}{j\pi}\int_\Omega u_{j,h}^{(i)} \Delta(\eta s_{-j}) dx, \quad j \in L. \tag{28}$$

TABLE 1. Standard FEM : The Case $\omega = \frac{3\pi}{2}$ for **Example 1**.

h	$\|u - u_{\text{SFEM}}\|_{L^2}$		$\|u - u_{\text{SFEM}}\|_{H^1}$	
1/4	2.46765E-01	ratio	1.86976E+00	ratio
1/8	1.25735E-01	0.97275	1.00751E+00	0.89206
1/16	7.86280E-02	0.67727	5.55122E-01	0.85992
1/32	4.91390E-02	0.67817	3.31498E-01	0.74380
1/64	3.04667E-02	0.68963	2.14560E-01	0.62762
1/128	1.91169E-02	0.67239	1.53364E-01	0.48442
1/256	1.20800E-02	0.66223	1.16145E-01	0.40103

TABLE 2. DSFM : The Case $\omega = \frac{3\pi}{2}$ for **Example 1**.

h	λ_{BD}	$\|u - u_{\text{DSFM}}\|_{L^2}$		$\|u - u_{\text{DSFM}}\|_{H^1}$	
1/4	-0.84491	2.19156E-01	ratio	1.96950E+00	ratio
1/8	0.79786	4.80179E-02	2.19032	1.23294E+00	0.67572
1/16	0.93744	1.58683E-02	1.59743	6.78013E-01	0.86272
1/32	0.98311	3.69430E-03	2.10277	3.58807E-01	0.91810
1/64	0.99528	9.82260E-04	1.91113	1.84002E-01	0.96349
1/128	0.99892	2.34049E-04	2.06930	9.07121E-02	1.02035
1/256	0.99971	5.82881E-05	2.00553	4.49938E-02	1.01157

5. Numerical Experiments

We consider two examples: with one on the L-shape domain and the other on an almost crack domain with mixed boundary conditions. The computational results will be given by using FreeFEM++ code([8]).

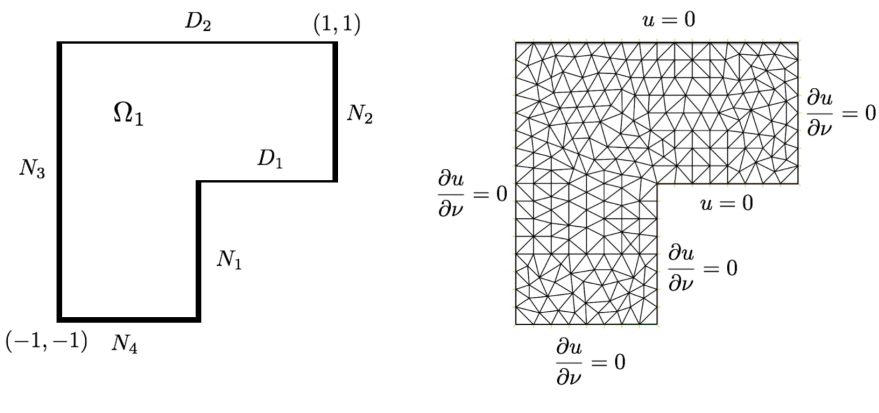

FIGURE 1. L-shape domain with mesh for Example 1.

5.1. Example 1. Consider a Poisson equation (1) in the L-shape domain $\Omega_1 = ((-1,-1) \times (1,1)) \backslash ([0,1) \times (-1,0])$, with $\Gamma_D = ((0,1) \times \{0\}) \cup ((-1,1) \times \{1\}) = D_1 \cup D_2$ and $\Gamma_N = \partial\Omega \backslash \Gamma_D = N_1 \cup N_2 \cup N_3 \cup N_4$ as in Figure 1.

TABLE 3. Our algorithm with $N = 1$: The Case $\omega = \frac{3\pi}{2}$ for **Example 1**.

h	$\lambda^{(0)}$	$\|u-u^{(1)}\|_{L^2}$		$\|u-u^{(1)}\|_{H^1}$	
1/4	-0.84491	4.34723E-01	ratio	2.08117E+00	ratio
1/8	0.79786	4.50666E-02	3.26997	9.43866E-01	1.14074
1/16	0.93744	1.40804E-02	1.67837	4.86763E-01	0.95536
1/32	0.98311	2.35463E-03	2.58011	2.35669E-01	1.04646
1/64	0.99528	6.24569E-04	1.91457	1.20646E-01	0.96598
1/128	0.99892	1.52077E-04	2.03806	5.98963E-02	1.01024
1/256	0.99971	3.92520E-05	1.95396	3.00458E-02	0.99531

TABLE 4. Our algorithm with $N = 2$: The Case $\omega = \frac{3\pi}{2}$ for **Example 1**.

h	$\lambda^{(1)}$	$\|u-u^{(2)}\|_{L^2}$		$\|u-u^{(2)}\|_{H^1}$	
1/4	-0.785380	4.23798E-01	ratio	2.07828E+00	ratio
1/8	0.798366	4.50292E-02	3.23444	9.43832E-01	1.13879
1/16	0.937380	1.40840E-02	1.67680	4.86768E-01	0.9553
1/32	0.983200	2.35470E-03	2.58045	2.35659E-01	1.04653
1/64	0.995326	6.24160E-04	1.91555	1.20640E-01	0.966
1/128	0.998943	1.51952E-04	2.03830	5.98918E-02	1.01027
1/256	0.999724	3.91789E-05	1.95547	3.00421E-02	0.99537

Note that the inner angle is $\omega = \frac{3\pi}{2}$ and the singular function is

$$s = s(r, \theta) = r^{\frac{1}{3}} \sin \frac{\theta}{3}.$$

The exact solution is given by $u_{\text{exact}} = \eta_{0.75}s + 3y^3 + 2y^2 - 5y$, so that the input function is $f = -\Delta(\eta_{0.75}s) - 18y - 4$.

In Table 1, 2, 3 and 4, we give the computational results by three algorithms: 1) standard FEM, 2) DSFM given in the subsection 3.3, and 3) our algorithms with $N = 1$ and 2, respectively.

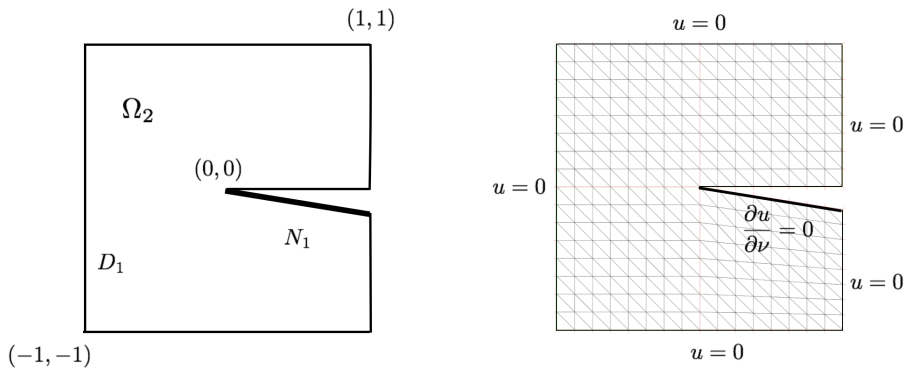

FIGURE 2. Domain and its mesh for Example 2.

TABLE 5. Standard FEM : The Case $\omega = \frac{39\pi}{20}$ for **Example 2**.

h	$\|u - u_{\text{SFEM}}\|_{L^2}$		$\|u - u_{\text{SFEM}}\|_{H^1}$	
1/4	2.11325E-01	ratio	1.87152	ratio
1/8	1.05863E-01	0.99727	1.15871	0.69169
1/16	6.12617E-02	0.78914	0.69622	0.73491
1/32	3.98885E-02	0.61901	0.45169	0.62419
1/64	2.71520E-02	0.55491	0.32560	0.47227
1/128	1.86719E-02	0.54019	0.25365	0.36025
1/256	1.29394E-02	0.52910	0.20595	0.30056

TABLE 6. DSFM : The Case $\omega = \frac{39\pi}{20}$ for **Example 2**.

h	$\lambda_{BD,1}$	$\lambda_{BD,3}$	$\|u - u_{\text{DSFM}}\|_{L^2}$		$\|u - u_{\text{DSFM}}\|_{H^1}$	
1/4	0.23835	0.36859	2.03082E-01	ratio	2.01337	ratio
1/8	0.72528	0.82065	8.02292E-02	1.33986	1.65080	0.28645
1/16	1.01487	0.95525	2.44261E-02	1.71570	1.00758	0.71227
1/32	1.04674	0.98894	6.87108E-03	1.82981	0.53495	0.91342
1/64	1.04547	0.99727	2.10963E-03	1.70355	0.27016	0.98559
1/128	1.03446	0.99941	7.68869E-04	1.45618	0.13477	1.00327
1/256	1.02469	0.99988	3.34263E-04	1.20175	0.0673861	1.00002

TABLE 7. Our algorithm with $N = 1$: The Case $\omega = \frac{39\pi}{20}$ for **Example 2**.

h	$\lambda_1^{(0)}$	$\lambda_3^{(0)}$	$\|u - u^{(1)}\|_{L^2}$		$\|u - u^{(1)}\|_{H^1}$	
1/4	0.23835	0.36859	1.88000E-01	ratio	1.84260E+00	ratio
1/8	0.72528	0.82065	5.63905E-02	1.74095	1.06591E+00	0.78966
1/16	1.01487	0.95525	1.33097E-02	2.08297	5.42950E-01	0.97319
1/32	1.04674	0.98894	3.80401E-03	1.80689	2.68317E-01	1.01688
1/64	1.04547	0.99727	1.41426E-03	1.42747	1.26153E-01	1.08876
1/128	1.03446	0.99941	6.58249E-04	1.10334	5.36991E-02	1.23220
1/256	1.02469	0.99988	3.18017E-04	1.04953	1.48306E-02	1.85632

5.2. Example 2. Consider a Poisson equation (1) on a domain $\Omega_2 = ((-1,-1) \times (1,1)) \setminus \left\{(x,y) : 0 \le x \le 1, -\tan(\frac{\pi}{20})\, x \le y \le 0\right\}$ as in Figure 2. Note that the inner angle $\omega = \frac{39\pi}{20}$, and the singular functions are given by

$$s_1 = s_1(r,\theta) = r^{\frac{10}{39}} \sin\frac{10\theta}{39} \quad \text{and} \quad s_3 = s_3(r,\theta) = r^{\frac{10}{13}} \sin\frac{10\theta}{13}.$$

Let $f = -\Delta(\eta_{0.75} s_1) - \Delta(\eta_{0.75} s_3)$ with the exact solution $u_{\text{exact}} = \eta_{0.75} s_1 + \eta_{0.75} s_3$.

We list the computational results in Table 5, 6, 7 and 8, from using three algorithms as in **Example 1.**

6. Conclusion

For the L-shaped domain problem, DSFM in the subsection 3.3 gives the optimal speed of convergence and our algorithm with either $N = 1$ or $N = 2$ give the optimal speed in L^2-norm and H^1-seminorm. So, we note that $N = 1$ is enough and that

TABLE 8. Our algorithm with $N = 2$: The Case $\omega = \frac{39\pi}{20}$ for **Example 2**.

h	$\lambda_1^{(1)}$	$\lambda_3^{(1)}$	$\|u-u^{(2)}\|_{L^2}$		$\|u-u^{(2)}\|_{H^1}$	
1/4	0.18510	0.35974	1.93311E-01	ratio	1.84864	ratio
1/8	0.58836	0.82353	6.39505E-02	1.59590	1.08339	0.77091
1/16	0.90148	0.95423	1.52319E-02	2.06986	5.61886E-01	0.94720
1/32	0.96636	0.98868	3.85761E-03	1.98132	2.86476E-01	0.97186
1/64	0.99057	0.99711	9.55834E-04	2.01288	1.43644E-01	0.99592
1/128	0.99695	0.99932	2.33957E-04	2.03052	7.14834E-02	1.00682
1/256	0.99892	0.99981	5.86432E-05	1.99621	3.57906E-02	0.99803

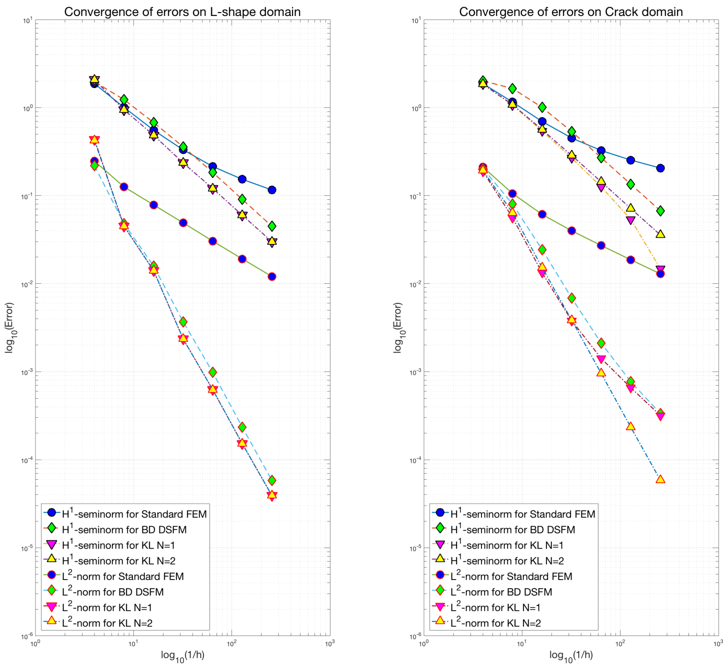

FIGURE 3. Convergences in the L^2-norm and H^1-seminorm of $u_{\text{exact}} - u_h$ on an L-shaped domain (left) and crack domain (right).

the errors obtained with our algorithm are smaller than those with the others in L^2-norm.

For the case of almost crack domain, both DSFM in the subsection 3.3 and our algorithm with $N = 1$, do not give the optimal speed of convergence in L^2-norm. But our algorithm with $N = 2$ gives the optimal convergence rate in L^2-norm and H^1-seminorm. Moreover, the errors obtained with our algorithm are smaller than those with the others in L^2-norm and H^1-seminorm. Figure 3 shows the convergence rates in L^2-norm and H^1-seminorm of $u_{\text{exact}} - u_h$ on an on an L-shaped domain and crack domain for four cases.

We conclude that our algorithm with $N = 2$ give optimal convergence for the Poisson problems with singularity raised by the mixed boundary condition with smaller errors than those of DSFM.

Acknowledgments

The first author was supported by Basic Science Research Program through the National Research Foundation of Korea (NRF-2014R1A1A2056734) and the second author was supported by Basic Science Research Program through the National Research Foundation of Korea (NRF-2016R1D1A1B03932219).

References

[1] T. Apel, Anisotropic finite elements: local estimates and applications, Teubner Stuttgart Leipzig,1999
[2] H. Blum and M. Dobrowolski, On finite element methods for elliptic equations on domains with corners, Computing, 28 (1982), 53-63.
[3] S. C. Brenner, Multigrid methods for the computation of singular solutions and stress intensity factor I: Corner singularities, Math. Comp., 68 (226), (1999), 559-583.
[4] Z. Cai and S.C. Kim, A finite element method using singular functions for the poisson equation: Corner singularities, SIAM J. Numer. Anal., 39:(2001), 286-299.
[5] Z. Cai , S.C. Kim, S.D. Kim, S. Kong, A finite element method using singular functions for Poisson equations: mixed boundary conditions, Comput. Methods Appl. Mech. Engrg. 195 (2006) 26352648
[6] M. Dauge, Elliptic boundary value problems on corner domains, Vol. 1341 of Lecture Notes in Mathematics. Springer-Verlag, Berlin, 1988.
[7] P. Grisvard, Elliptic Problems in Nonsmooth Domains, Pitman, Boston, MA, 1985.
[8] F. Hecht, New development in FreeFem++, J. Numer. Math. 20 (2012), no. 3-4, 251265.
[9] K.-Y. Kim and H.-C. Lee, A posteriori error estimators for nonconforming finite element methods of the linear elasticity problem, Journal of Computational and Applied Mathematics, 235(2010) 186-202.
[10] H.-C. Lee and K.-Y. Kim, A posteriori error estimators for stabilized $P1$ nonconforming approximation of the Stokes problem, Compt. Methods Appl. Mech. Engrg., 199(2010) 2903-2912.
[11] S. Kim and H.-C. Lee, A finite element method for computing accurate solutions for Poisson equations with corner singularities using the stress intensity factor, Computers and Mathematics with Applications, 71(2016) 2330-2337.
[12] S. Kim and S. Kong, Remarks on finite element methods for corner singularities using SIF, Honam Mathematical J., 38(2016), No.3, 661-674.
[13] H. Li, A. Mazzucato, V. Nistor, Analysis of the Finite Element Method for transmission/mixed boundary value problems on general polygonal domains, Electronic Transactions on Numerical Analysis, 37: 41-69, 2010.
[14] A. Quarteroni and A. Valli, Numerical Approximation of Partial Differential Equations, Springer-Verlag, Berlin, Germany, 1994.
[15] G. Raugel, Resolution numerique par une methode delements finis du probleme de Dirichlet pour le Laplacien dans un polygone, C. R. Acad. Sci. Paris Ser. A-B, 286 (1978), 791-794.
[16] A. Schatz and L. Wahlbin, Maximum norm estimates in the finite element method on plane polygonal domains, Part 1, Math. Comp., 32 (1978), 73109.
[17] Z. Yosibash, Singularities in elliptic boundary value problems and elasticity and their connection with failure initiation, Interdisciplinary Applied Mathematics, 37. Springer, New York, 2012.

Department of Mathematics, Changwon National University, Changwon, 51140, Republic of Korea.
E-mail: `sckim@changwon.ac.kr`

Department of Mathematics, Ajou University, Suwon, 16499, Republic of Korea.
E-mail: `hclee@ajou.ac.kr`